A Method of Calibrating Magnetometers on a Spinning Spacecraft

W. M. Farrell, R. F. Thompson, R. P. Lepping, and J. B. Byrnes

Abstract—**This paper describes a procedure for quantifying and compensating for angular offsets and slow-varying drifts associated with a flux-gate magnetometer onboard a spinning spacecraft. Such magnetometers have been flown on numerous spacecraft such as IMP-8, DE-1, and ISTP/GEOTAIL, and similar instruments are currently proposed to fly on the ISTP/WIND spacecraft. Consequently, slight geometric misalignment of the sensor from their chosen axes will create errors in the measured signal. These misalignments can be quantified using perturbation theory and compensated in the data analysis process. The technique is applicable to magnetometers on spinning spacecraft. Also, over long time periods, the magnetometer will develop slight drifts in the electronic components, and these too can be quantified in the data analysis process. We shall discuss a technique that quantifies and compensates for such perturbations from the measurements. The technique has been successfully applied for the last sixteen years to IMP-8 magnetometer data and more currently to the GEOTAIL magnetometer data, and can be applied in a general way to measurements from any magnetometer onboard a spinning spacecraft. Further improvements in the technique will also be discussed.**

I. Introduction

MAGNETOMETERS used in space science applications commonly suffer from two sources of error; one type resulting from slight sensor misalignments with respect to the coordinate axis, and the other from drifts in the quiescent point of the electronic components. For example, the drifts in the zero levels of the IMP-7 magnetometer system were on the order of a nanoTesla over the two year operation period of the instrument [1], while the electronic drifts associated with the HEOS-2 magnetometer were also on the order of a nanoTesla over a four year period [2]. Although such errors seem relatively insignificant, they must be quantified and compensated for in order to ensure an accurate measurement of the ambient magnetic field.

The two types of errors can be identified in the magnetometer measurements onboard a spinning spacecraft. The errors can be removed using a dual-magnetometer system, each possessing a triad of (nearly) orthogonal sensors. Such systems are currently flown on IMP-8, DE-1, and ISTP/GEOTAIL and are proposed to be flown on the ISTP/WIND spacecraft.

Manuscript received April 29, 1993; revised August 9, 1994.

The authors are with Laboratory for Extraterrestrial Physics, NASA/Goddard Space Flight Center, Greenbelt, MD 20771.

IEEE Log Number 9407896.

We will describe a procedure to identify and remove the sensor errors resulting from misalignments and electronic drifts from an instrument onboard a spinning spacecraft. The technique has been in successful use for over 16 years as part of the standard processing of the IMP-8 magnetometer data. Further, the concepts discussed here can be applied, in a general way, to magnetometers flown on any spinning spacecraft.

It should be recognized that our error removal technique is distinctly different from those previously discussed [2], [3]. These other techniques make use of "Alfvenic" type changes in the ambient magnetic field (i.e., changes in field direction rather than magnitude) that then allow a statistical determination of the sensor error. Such techniques have the advantage of applicability to a spinning or nonspinning spacecraft. However, the technique is valid only in regions where most the field changes can be considered "Alfvenic." In other words, the spacecraft has to be in the interplanetary magnetic field (IMF) for application. Also, these alternative techniques cannot differentiate between an error in misalignment or electronic drift; both types of error are measured together. The technique we are about to describe for spinning spacecraft can be applied in any region of space and clearly separates the two types of errors.

II. System Definition

Before the method is described in detail, the geometry of the magnetometer and spacecraft systems should be defined. In particular, there are two coordinate systems involved in the data analysis, and these are shown in Fig. 1. Consider a spin-stabilized spacecraft rotating about the **Z**-axis with angular frequency, ω. The plane normal to this axis is commonly referred to as the "spin-plane," and is defined by the orthogonal "apparent" coordinate vectors **XA** and **YA** that rotate about **Z** at ω. The vector **ZA** = **Z** forms a third orthogonal basis vector of this system. A vector, **R,** in the apparent system transforms to the non-rotating, inertially-fixed "payload" coordinate system by the transformation, Ω^{-1} defined as:

$$\begin{bmatrix} R_{XP} \\ R_{YP} \\ R_{ZP} \end{bmatrix} = \begin{bmatrix} \cos(\omega t) & -\sin(\omega t) & 0 \\ \sin(\omega t) & \cos(\omega t) & 0 \\ 0 & 0 & 1 \end{bmatrix} \begin{bmatrix} R_{XA} \\ R_{YA} \\ R_{ZA} \end{bmatrix}. \quad (1)$$

The vector **XP** in this case is defined as the projection of the vector pointing to the sun, **YP** is orthogonal to **XP**

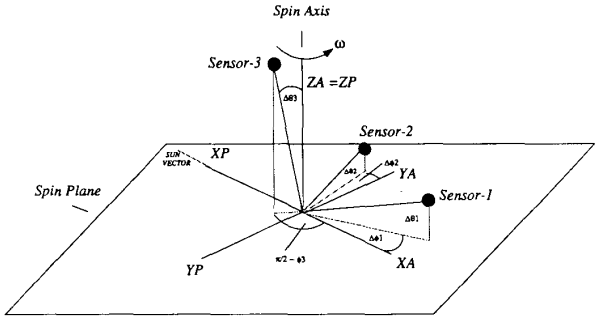

Fig. 1. The geometry of the magnetometer system. Note that the sensors and apparent coordinate system (*XA, YA, ZA*) all rotate at the spin frequency, ω. In contrast, the payload coordinate system (*XP, YP, ZP*) is inertially-defined.

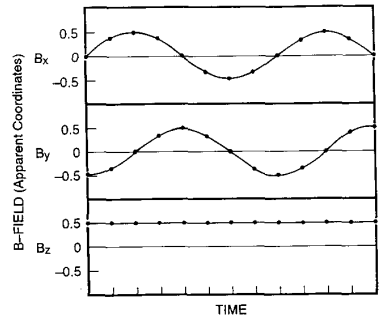

Fig. 2. The signals detected from ideally-aligned sensors.

and in the spin plane, while **ZP** = **Z** forms the third orthogonal basis vector of this system.

III. Ideal Alignment

Consider an inertially-defined magnetic field vector, **B**, with component B_z projected along the spin axis and component B_{sp} projected into the spin plane. Also, consider that each of the magnetic sensors of a flux-gate magnetometer lie parallel to each of the apparent coordinate axis, **XA, YA,** and **ZA** (corresponding to a perfectly aligned system in Fig. 1, with all $\Delta\theta$ and $\Delta\phi$ set to zero). In this "ideal" configuration, there will be no spin-modulated component in the ZA-sensor, and a strong spin-modulated component will be present in the XA and YA sensors. Further, in this configuration, the phase difference between the spin-modulated signals nmeasured by XA-sensor and YA-sensor will be exactly 90°. The "apparent" **B** measured by the sensors is shown in Fig. 2. As indicated in the figure, the measurements in the spin-plane oscillate about a "true" zero-level. The simple transformation defined in (1) can then be used to obtain **B** in payload coordinates. Since the sensors are assumed to be exactly aligned with the apparent coordinate axis, no vestige of spin-modulation will remain in the signal upon transforming. In other words, the transformation defined in (1) will eliminate all spin-modulation when sensors are ideally-aligned.

Unfortunately, the magnetic sensors are rarely aligned perfectly along the chosen coordinate axis. Also, over long periods of time, the "true" zero level will tend to drift due to slight changes in the magnetometer electrical system. However, these deviations from ideal magnetometer behavior can be quantified and eliminated in the data processing stage, and a method to do this will be described in the following sections.

IV. Effects of Small Misalignments

Imagine that the magnetometer sensor initially intended to be aligned with the **XA** coordinate was shifted slightly in both azimuth ($\Delta\phi_1$) and elevation ($\Delta\theta_1$), as shown in Fig. 1. We shall define this sensor as "1." Such a misalignment in Sensor-1 results in three observed perturbations in the signal:

1) The magnitude of the spin-plane component of B, B_{sp}, is slightly underestimated by the sensor as compared to the actual value of B_{sp}.
2) The spin-phasing of B_{sp} is shifted slightly relative to an "ideal" sensor alignment.
3) The zero-level (or dc offset) of the sensor is shifted relative to the perfectly aligned sensor.

As we shall soon derive, a similar set of perturbations will arise in a misaligned sensor intended to lie along **YA** (Sensor-2). For a misaligned sensor intended to lie along the **ZA** axis (like Sensor-3 in Fig. 1), two perturbations in the signal will result:

1) The magnitude of the spin-axis component of B, B_Z, is slightly underestimated as compared to its real value.
2) Spin-modulation develops in the signal, that would not be present in a perfectly aligned sensor.

Changes in the sensor zero level occurring from electronic drifts will add a constant value to the magnetic field that is uncorrelated with magnetometer position. To demonstrate how these perturbations develop, we shall estimate the magnetic field value measured by the misaligned sensor, and compare it to the value measure by a perfectly-aligned sensor.

In a very general way, the direction of Sensor-1, $\mathbf{R_1}$, can be written as

$$\mathbf{R_1} = (\sin\theta_1 \cos\phi_1, \sin\theta_1 \sin\phi_1, \cos\theta_1), \qquad (2)$$

in the apparent coordinate system (i.e., XA, YA, & ZA). The quantity θ_1 represents the sensor's angular orientation relative to the spin axis, while ϕ_1 represents the sensor's azimuth angle relative to the **XA** axis. For ideal placement,

$$\theta_1 = 90°$$

and

$$\phi_1 = 0°, \qquad (3)$$

making

$$\mathbf{R_1} = (1, 0, 0). \tag{4}$$

For a misalignment in elevation, $\Delta\theta_1$, and azimuth, $\Delta\phi_1$, like those shown in Fig. 1, the angles become

$$\theta_1 = 90° - \Delta\theta_1$$

and

$$\phi_1 = \Delta\phi_1, \tag{5}$$

with the perturbations being either positive or negative in value. Assuming only small misalignments of the sensors, the trigonometric terms can be approximated by

$$\cos\theta_1 = \cos(90° - \Delta\theta_1) \sim \Delta\theta_1,$$

$$\sin\theta_1 = \sin(90° - \Delta\theta_1) \sim 1 - (\Delta\theta_1)^2/2,$$

$$\cos\phi_1 = \cos(\Delta\phi_1) \sim 1 - (\Delta\phi_1)^2/2,$$

and

$$\sin\phi_1 \sim \Delta_1. \tag{6}$$

Hence, to the second-order, the misaligned sensor position becomes

$$\mathbf{R_1} = (1 - \epsilon_1, \Delta\phi_1, \Delta\theta_1), \tag{7}$$

where $\epsilon_1 = (\Delta\theta_1^2 + \Delta\phi_1^2)/2$.

In the frame of reference of the spinning spacecraft (the "apparent" coordinate system) a general form of the magnetic field vector can be written using the inverse of the tensor shown in (1):

$$B_{XA} = B_{SP}\cos(\omega t - \psi),$$

$$B_{YA} = -B_{SP}\sin(\omega t - \psi),$$

and

$$B_{ZA} = B_{ZP} = B_Z, \tag{8}$$

where $B_{SP} = (B_{XP}^2 + B_{YP}^2)^{1/2}$ and $\psi = \tan^{-1}(B_{YP}/B_{XP})$. For the sake of demonstration, we assume that **B** lies in the *XP*/*ZP* plane, so that $\psi = 0$ at $t = 0$. This assumption can be made without any loss of generality, since only a phase shift ψ is required to describe B fields out of this plane (ωt changes to $\omega t \rightarrow \omega t - \psi$ in the following equations). Given B in the *XP*/*ZP* plane, a misaligned Sensor-1 will then detect a magnetic field of

$$\mathbf{B}\cdot\mathbf{R_1} \sim (1 - \epsilon_1)B_{SP}\cos\omega t - \Delta\phi_1 B_{SP} \cdot \sin\omega t + \Delta\theta_1 B_Z + B_{1\text{-elec}}. \tag{9}$$

The quantity $B_{1\text{-elec}}$ represents the change in measurement due to any electronic drifts. For comparison, a perfectly aligned sensor (without drifts) will detect a signal of

$$\mathbf{B}\cdot\mathbf{R_1} = B_{SP}\cos\omega t. \tag{10}$$

Thus, a misaligned sensor will create a number of perturbations to the measured signal. There is both a time dependent contribution:

$$\Delta B(t) \sim -B_{SP}(\epsilon_1\cos\omega t + \Delta\phi_1\sin\omega t) \tag{11}$$

and a quasi-dc contribution:

$$\Delta B \sim \Delta\theta_1 B_Z + B_{1\text{-elec}}. \tag{12}$$

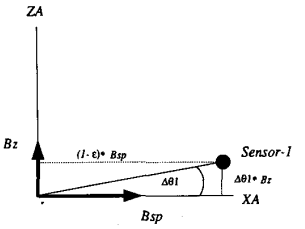

Fig. 3. The effect of an elevated sensor out of the spin plane. Note that a projection of B along the spin-axis (B_Z) is measured by the elevated sensor.

Equation (11) possess a decrease in magnitude and phase shift in the measured spin-plane component of B, B_{SP}. Since the sensor is shifted slightly out of the spin plane, it detects a reduced B_{SP} component, while the displacement in azimuth, $\Delta\phi$, is the sole source of the phase shift. Due to the elevation out of the spin plane, the sensor now detects a projection of the constant B_Z component, which accounts for the zero-level offset in (12) (see Fig. (3)).

For a misaligned sensor (Sensor-2) along the **YA** axis, a similar equation can be derived using $\theta_2 = 90° - \Delta\theta_2$ and $\phi_2 = 90° + \Delta\phi_2$:

$$\mathbf{B}\cdot\mathbf{R_2} \sim \Delta\phi_2 B_{SP}\cos\omega t - (1 - \epsilon_2)B_{SP} \cdot \sin\omega t + \Delta\theta_2 B_Z + B_{2\text{-elec}}, \tag{13}$$

where $\epsilon_2 = (\Delta\theta_2^2 + \Delta\phi_2^2)/2$ and the label "2" indicates the second sensor of the magnetometer. For perfect alignment:

$$\mathbf{B}\cdot\mathbf{R_2} = -B_{SP}\sin\omega t. \tag{14}$$

Comparing expressions (9) and (13), it is evident that the Sensor-2 perturbations are similar in nature to those of Sensor-1. Basically, a smaller magnitude and phase shift are measured for B_{SP}, along with a dc offset.

A sensor perfectly-aligned along the **ZA** axis will detect only a constant B value, without any spin modulation. However, if the sensor is misaligned, then a spin-modulated component will be observed. In general, the position of the spin-aligned sensor, Sensor-3, can be written as

$$\mathbf{R_3} = (\sin\theta_3\cos\phi_3, \sin\theta_3\sin\phi_3, \cos\theta_3). \tag{15}$$

The misalignment consists of a tilt from the **ZA** axis, this directed along the (arbitrary) azimuth angle ϕ_3. The geometry is illustrated in Fig. 1. The tilt and azimuth angles can be written as

$$\theta_3 = \Delta\theta_3$$

and

$$\phi_3 = \phi_3. \tag{16}$$

For small misalignments,

$$\cos\theta_3 \sim 1 - (\Delta\theta_3)^2/2$$
$$\sin\theta_3 \sim \Delta\theta_3$$
$$\cos\phi_3 = \cos\phi_3$$
$$\sin\phi_3 = \sin\phi_3 \qquad (17)$$

Hence, the second-order position vector of the sensor is

$$\mathbf{R_3} = (\Delta\theta_3 \cos\phi_3, \Delta\theta_3 \sin\phi_3, 1 - \epsilon_3) \qquad (18)$$

where $\epsilon_3 = \Delta\theta_3^2/2$. The magnetic field measured by Sensor-3 is then

$$\mathbf{B} \cdot \mathbf{R_3} \sim \Delta\theta_3 \cos\phi_3 B_{SP} \cos\omega t - \Delta\theta_3 \sin\phi_3 B_{SP} \sin\omega t + (1 - \epsilon_3) B_z + B_{z\text{-}elec} \qquad (19)$$

$$\boxed{\mathbf{B} \cdot \mathbf{R_3} \sim \Delta\theta_3 B_{SP} \cos(\omega t + \phi_3) + (1 - \epsilon_3) B_Z + B_{z\text{-}elec}.} \qquad (20)$$

Note that the measured field for a perfectly aligned sensor is

$$\mathbf{B} \cdot \mathbf{R_3} = B_z. \qquad (21)$$

Thus, a slight misalignment of a sensor, intended to lie along **ZA,** results in an added spin-modulation to the signal that would not normally be present, along with a slight reduction in the value of the B_z component measured by the sensor.

Fig. 4 is similar to Fig. 2, in that it illustrates the measured magnetic field signals from the three sensors, but now the effects from the sensor misalignments described above are included. Note that a DC offset, phase shift, and reduced value are associated with measurements from the spin-plane sensors. The spin-aligned sensor now has a spin-modulated component to the signal that would not normally be present in the ideal case. This is a pictorial example of the types of perturbations expected from misaligned sensors.

V. Quantifying the Perturbations

Fortunately, information about the misalignments of each sensor is contained in the time-series data. These data should then be analyzed before final processing to (a) obtain the degree of misalignment and zero-level drift and (b) correct for such effects. We shall now describe a method to do both. The method is based upon the assumption that the misalignment of the Sensor-3, that along the **ZA** axis, is small ($\Delta\theta_3 << 1$). In other words, this sensor is assumed to be only slightly tilted from the spin axis. Under most circumstances, this is a very safe assumption. We can then correlate the B_z signal measured by the (nearly) spin-aligned sensor to the projection of B_z detected by the spin-plane sensors (i.e., B_z resulting from the misalignments, as described in (9) and (13)). From this correlation, the spin-plane sensor's functional dependence on elevation angle, $\Delta\theta$, can be obtained and corrected. Also, the spin-modulated component to the spin-aligned sensor can be quantified and corrected. Note that the sensor triad does not have to be orthogonal in order for the method to work. The quantities $\Delta\theta_1$ and $\Delta\theta_2$ are calculated independently without assuming an intersensor orthogonality. The only required assumption is that $\Delta\theta_3$ remains small. This method will allow us to reconstruct the field values as if the sensors were not misaligned.

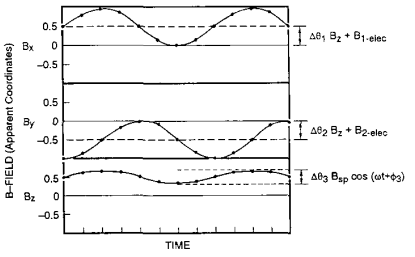

Fig. 4. The signals detected from sensors misaligned as described in the text.

To determine the misalignment in the spin-plane sensors (Sensors 1 and 2 intended to lie along the **XA** and **YA** axis, respectively), the following analysis, called the "Slope-Intercept" method, can be performed:

a) The data from Sensor-1 (supposedly **XA** aligned) taken over a time interval of several spin periods (a minimum of 1 to many tens) is run through a trigonometric spin fit routine that determines the coefficients (C_0^1, C_1^1, C_2^1) of the function

$$F(t) = C_0^1 + C_1^1 \sin\omega t' + C_2^1 \cos\omega t' \quad \text{(counts)}, \qquad (22)$$

where $t' = t - t_{\text{sun}}$, t_{sun} being the time the **XA** axis crosses the spin-plane projection of the vector pointing to the sun (or, by definition, the **XP** axis). The phase of the **XA** axis relative to the sun vector is often referred to as the "sun phase." It is assumed that the data has little noise and that the field is not changing dramatically over the fitting interval. If the sensor was perfectly aligneed, C_0^1 would represent the "true" zero-level. However, any misalignments will alter these zero-level values. This analysis is repeated over successive time intervals in order to obtain a large set of C^1s. It should be noted that the dc offset and time dependent coefficients can also be derived by performing Fourier transform spectral analysis.

b) The same spin-fit routine is applied to the data obtained from Sensor-2 in time intervals similar to that used for Sensor-1. Like the previous case, a large set of C_0^2, C_1^2, and C_2^2 values are collected.

c) The same spin-fit routine is applied to the data obtained from Sensor-3 in similar time intervals as the previous two sensors. Again, a large set of C_0^3, C_1^3, and C_2^3 values are collected. It is assumed that the sensor is only slightly misaligned, hence $C_0^3 > C_1^3, C_2^3$.

d) Given a large number of time intervals (enough intervals so that B_z is allowed to vary as a function time), the parameters C_0^1 and C_0^2 can now be correlated to C_0^3 by performing a least-squares linear fit to the set of values

(C_0^3, C_0^1) and (C_0^3, C_0^2). It is assumed that C_0^1 and C_0^2 relate to C_0^3 by

$$C_0^1 = \text{SLOPE}_x * C_0^3 + \text{INTERCEPT}_x$$

and

$$C_0^2 = \text{SLOPE}_y * C_0^3 + \text{INTERCEPT}_y. \quad (23)$$

In this notation, the intercept values represent the zero level of the sensor while the slope is directly proportional to the misalignment angle.

The INTERCEPT values determine the zero level at the time of measurement. Hence, the electronic drift in the sensor can be quantified by comparing these values to those obtained during preflight calibration. Thus, $B_{1\text{-elec}}$ and $B_{2\text{-elec}}$ are derived from these INTERCEPTs.

Using this procedure, we have quantified the dc offset, phase position, and the zero level for Sensor 1 and 2. We shall now describe the analysis for the spin-aligned sensor, Sensor-3, called the "Beta-Phi" method:

a) The sensor's azimuthal displacement from the **XA** axis, ϕ_3, is determined from

$$\phi_3 = \tan^{-1}(C_1^3/C_2^3) - \tan^{-1}(C_1^1/C_2^1) \quad (24)$$

b) The tilt-angle, $\Delta\theta_3$, is determined from comparing the B_{SP} component measured by the misaligned Sensor-3 (i.e., $\sim((C_1^3)^2 + (C_2^3)^2)^{1/2}$) to the B_{SP} component measured by the spin-plane sensors, $B_{SP} = (B_1^2 + B_2^2)^{1/2}$, where B_1 and B_2 represent the field strength measured in Sensor-1 and -2 (with the erroneous dc offsets removed to improve the accuracy). The angle $\Delta\theta_3$ is then:

$$\Delta\theta_3 = \sin^{-1}(S^3((C_1^3)^2 + (C_2^3)^2)^{1/2}/B_{SP}). \quad (25)$$

The quantity S^3 represents the sensor sensitivity (conversion from counts to gammas). Note that the true B-field values are used to determine this particular angle.

d) Unfortunately, for the magnetometers onboard WIND and GEOTAIL, the "true" sensor zero level of Sensor-3, that along **ZA,** cannot be determined directly. Normally, the spin-aligned sensor would be flipped into the spin plane, as was done with IMP-8, to allow the "true" zero-level to be determined in the same manner as described above (i.e., slope/intercept method). However, such flipping will not be done on the WIND and GEOTAIL experiments. To determine this one quantity, the "true" zero level of Sensor-3, we shall then apply the other techniques [2], [3].

VI. Removing the Perturbations

Using the parameters from the "Slope/Intercept" and "Beta/Phi" methods, the effects of the sensor misalignments can be determined from the measurements. These misalignments can then be removed and the transformation to payload coordinates can then be made using the tensor in Eq. (1). We shall first discuss the analysis that was performed on the IMP-8 data, and then discuss possible improvements that might be incorporated into the WIND magnetometer data analysis.

IMP-8 Processing. Only the dc offsets of the spin plane sensors (i.e., $\Delta\theta B_Z$ term in equations (9) and (13)) are considered in the IMP-8 magnetometer processing system. It is assumed that the perturbations ϵ and $\Delta\phi$ are small. In other words, the slightly reduced magnitude and altered phase in the measured B_{SP} signal are neglected, and only the effect of the projection of B_Z is currently considered. For Sensor-3, the spin-aligned sensor, the added spin-modulation from misalignment is eliminated by subtracting $\Delta\theta_3 B_{SP} \cos(\omega t + \phi_3)$ from the measured Sensor-3 signal. It is again assumed that ϵ in (20) is small, and thus can be neglected. The removal of the perturbations included the following steps:

(a) To remove the dc zero-level offset, the value

$$\text{DELTA}_x = \text{SLOPE}_x * C_0^3, \quad (26)$$

is subtracted from the Sensor-1 measurement and

$$\text{DELTA}_y = \text{SLOPE}_y * C_0^3, \quad (27)$$

is subtracted from the Sensor-2 measurement. The SLOPE and INTERCEPT values are calculated using the linear fit routine described in the previous section.

b) The spin-dependent perturbation in the Sensor-3 measurements is removed by subtracting $\Delta\theta_3 B_{SP} \cos(\omega t + \phi_3)$ from the measurements. The values of $\Delta\theta_3$ and ϕ_3 were obtained from the method described previously. The value of B_{SP} is obtained from geometric mean of the values of Sensor-1 and Sensor-2 with the erroneous zero-levels removed: $B_{SP} = (B_1^2 + B_2^2)^{1/2}$.

As mentioned previously, for the sake of the arguments above, we have placed **B** in the **XP/ZP** plane. This makes the formalism accurate up to a phase shift, ψ (see Section IV). For an arbitrary magnetic field direction, the phasing of the signal becomes

$$\omega t \rightarrow \omega t - \psi \quad (28)$$

where ψ is the angle of B_{SP} in the spin plane. Fig. 5 shows the geometry for B_{SP} located in an arbitrary azimuth position. Note in the figure that ψ is the angle between B_{SP} and the inertially-defined **XP** axis, while σ is the angle between B_{SP} and the spinning **XA** axis. Hence, the azimuth angle between B_{SP} and the spin plane projection of Sensor-3 becomes

$$\omega t - \psi + \phi_3 = -\sigma + \phi_3 = \phi_3 - \sigma \quad (29)$$

where $\sigma = \tan^{-1}(B_2/B_1)$. This angle defines the position of B_{SP} in the **XA/YA** plane. Since the apparent coordinate system is spinning with the spacecraft and B is inertially fixed, σ will range through all angular values (0° to 360°) every spin period. The spin-modulated component of Sensor-3, created by misalignment, is

$$\Delta\theta_3 B_{SP} \cos(\phi_3 - \sigma) \quad (30)$$

and this component is subtracted from the Sensor-3 measurements.

With these first-order errors removed, the measurements are then transformed to payload coordinates using the simple rotation about the **ZA** axis shown in (1). Fur-

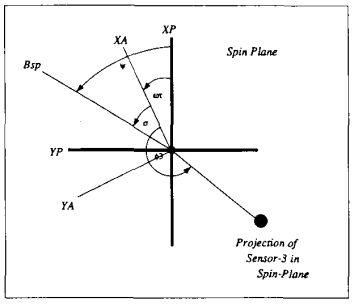

Fig. 5. The azimuth angles of various quantities in the spin plane.

ther analysis of these measurements, such as transforming to GSE and GSM coordinates and averaging can then be performed.

Possible Improvements. As stated previously, the ϵ and $\Delta\phi$ perturbations described in (2) to (21) are not eliminated from the measurements in an IMP-8 type analysis scenario. These terms could be removed to improve the accuracy of the measurement. This is particularly true of the $\Delta\phi$ terms, which are first-order perturbations, and thus have the potential to become very significant (possibly of equal significance to the first-order zero-level offsets, $\Delta\theta$ B_Z). In contrast, the ϵ terms are second-order and thus of less significance.

a) The azimuth offsets of the sensors, $\Delta\phi_{1,2}$ are actually difficult to quantify directly. This difficulty arises because only the total phase difference between Sensor-1 and Sensor-2 is measured, $\Delta\phi_{\mathrm{TOT}}$, and not the individual misalignments, $\Delta\phi_{1,2}$. The total phase difference, $\Delta\phi_{\mathrm{TOT}}$, is defined as

$$\Delta\phi_{\mathrm{TOT}} = \tan^{-1}(C_1^2/C_2^2) - \tan^{-1}(C_1^1/C_2^1) = 90^\circ + \Delta\phi_2 - \Delta\phi_1. \quad (31)$$

Before launch (i.e., prelaunch), the inter-orthgonality of the three magnetometer sensors (sensor triad) is measured, and the azimuthal offset angle, $\Delta\phi_1^{\mathrm{PRE}}$ and $\Delta\phi_2^{\mathrm{PRE}}$, are determined at this time. Usually, an interorthogonality offset matrix based on preflight measurements is provided by the investigator, and these small misalignments are then removed prior to calibration.

However, during the flight there may be periods when the azimuthal offsets deviate from their initial alignment. The most probable offset would involve the azimuthally bending on the boom. Since the spin-plane sensors (Sensor-1 and Sensor-2) are fixed on the boom, both see the same azimuthal offset from boom bending in their measurements: $\Delta\phi_1 = \Delta\phi_2 = \Delta\phi$.

The easiest way to quantify boom bending is to make use of measurements from a dual magnetometer system. In such an experiment, there are two separate magnetometers located at different points on the same boom. The purpose of such a system is to quantify the spacecraft field [4]. However, we can also apply the measurements to quantify $\Delta\phi$. As illustrated in Figure 6, the spin phase

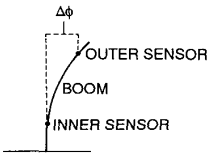

Fig. 6. Azimuthal bending of the magnetometer boom. For two separate magnetometers on the boom, a spin phase shift will be present which is related to $\Delta\phi$.

difference between the inner and outer magnetometers yields a zero-order estimate of the amount of boom bending. It is assumed that the inner magnetometer is located close to the spacecraft, and thus suffers little from the bending ($\Delta\phi_{\mathrm{INNER}} \sim 0$). Thus, the spin phase of this sensor is considered the true phase. In contrast, the outer magnetometer is shifted azimuthally, which results in a measured spin phase difference with respect to the inner magnetometer. This phase difference thus corresponds to $\Delta\phi_{\mathrm{OUTER}} \sim \Delta\phi$, where $\Delta\phi$ approximately represents the amount of boom bending.

To remove the effect of bending from the outer magnetometer, we need to recognize that $B_{SP} \sin \omega t$ is the field measured in Sensor-2, B_2, while $B_{SP} \cos \omega t$ is the field measured in Sensor-1, B_1. Thus, to remove the effects of bending (see (9) and (13)), add

$$\Delta\phi\ B_2 \quad (32)$$

to the Sensor-1 measurements and

$$\Delta\phi\ B_1 \quad (33)$$

to the Sensor-2 measurements.

b) Finally, the ϵ values in (9), (13), (20) can be completely quantified. These variables are $\epsilon_{1,2} = (\Delta\theta_{1,2}^2 + \Delta\phi_{1,2}^2)/2$ and $\epsilon_3 = \Delta\theta_3^2/2$. The $\Delta\theta_{1,2}$ values used in $\epsilon_{1,2}$ are derivable from the SLOPE-X and SLOPE-Y values:

$$\Delta\theta_{1,2} = \mathrm{SLOPE\text{-}X,Y}/S^3 \quad (34)$$

where S^3 is defined as the sensitivity value of Sensor-3 that converts counts to gammas. Thus, to remove these second-order effects from the sensor measurements, add

$$\epsilon_1 B_1,$$

$$\epsilon_2 B_2,$$

and

$$\epsilon_3 B_3 \quad (35)$$

to the values obtained in Sensor-1, Sensor-2 and Sensor-3, respectively.

At this point in the processing, the measurements should appear as if they were obtained by an ideally-aligned set of sensors. The transformation to payload coordinates, defined in (1), can now be made, creating measurements with little vestigial spin modulation. Further analysis such as transforming to inertial coordinate systems and averaging can now proceed.

VII. Conclusions

A method has been outlined that removes perturbations in magnetometer signals resulting from small sensor misalignments. The method works on any spinning spacecraft and, with the new additions to the procedure, may prove to be very accurate. Further, the method is relatively fast, allowing the zero-levels of the sensors to be determined in a comparatively short period of time. Many of the first-order perturbations are removed using the technique developed for the IMP-8 spacecraft. In the current version of the method, other first- and second-order perturbations can be quantified by the spin-fitting procedure and removed. This method will be used in the data analysis of the WIND magnetometer experiment, and is in current successful use in the GEOTAIL magnetometer data analysis.

The magnetometer calibration includes the following steps:

a) Run the raw data from all three sensors through a trigonometric spin fit routine or FFT spectral analysis routine to obtain the outputs C_0, C_1, and C_2 defined by (22).

Spin-Plane Sensor Analysis

b) Perform a linear fit of the spin-plane sensor (Sensor-1 & -2) $C_0^{1,2}$ values to the spin-axis (Sensor-3) C_0^3 values. Obtain the outputs SLOPE-X, SLOPE-Y, INTERCEPT-X, and INTERCEPT-Y.

c) Subtract erroneous zero-levels from spin-plane sensors (Sensor-1 & -2) using the newly-derived SLOPE-X, SLOPE-Y, INTERCEPT-X, and INTERCEPT-Y.

d) Remove phase shift resulting from $\Delta\phi_{1,2}$ and magnitude reduction resulting from $\epsilon_{1,2}$ from the spin-plane sensors (Sensor-1 & -2).

e) Compare INTERCEPT-X,Y values (zero-level) to preflight zero-levels to determine the amount of electronic drift that has occurred in the measurement.

Spin-Axis Sensor Analysis

f) Quantify the tilt angle, $\Delta\theta$, and azimuth position, ϕ, of the spin-axis sensor (Sensor-3).

g) Remove the spin-modulated term from the Sensor-3 measurements. The new output is B_3 with $\Delta\theta_3 B_{SP} \cos(\phi_3 - \sigma)$ removed.

h) Remove $\epsilon_3 B_3$ from the Sensor-3 measurements.

i) Transform the calibrated B-field values from apparent to payload coordinates. Since the values have the perturbations resulting from misalignments removed, the vestigial spin modulation is drastically reduced.

References

[1] W. H. Mish and R. P. Lepping, "Magnetic-Field Experiment Data Processing Systems, Explorers 47 and 50," Internal Report, NASA/GSFC, 1976.

[2] P. C. Hedgecock, "A correlation technique for magnetometer zero-level determination," *Space. Sci. Inst.*, vol. 1, pp. 83–90, 1975.

[3] J. W. Belcher, "A variation of the Davis-Smith method for in-flight determination of spacecraft magnetic fields," *J. Geophys. Res.*, vol. 78, pp. 6480-6490, 1973.

[4] N. F. Ness, "Magnetometers for space research," *Space Sci. Rev.*, vol. 11, pp. 459-554, 1970.

William M. Farrell received the B.S., M.S., and Ph.D. degrees from the University of Iowa.

He is a space scientist at the NASA Goddard Space Flight Center. He is a coinvestigator on the WIND magnetometer and radio wave experiments, the Cassini radio wave experiment, and a guest investigator on the Voyager radio astronomy experiment. His research interests include the building of magnetic antennae, radio signals from lightning, and planetary magnetic fields.

Richard F. Thompson received the B.S.E.E. degree from the University of Maryland, with particular emphasis on applied mathematics.

He has been a mathematican at the NASA Goddard Space Flight Center since 1970, and is currently investigating computational problems associated with atmospheric radiative transfer and chemical kinetics. He has been involved in the analysis of many scientific experiments flown in space, including the Voyager magnetometer experiment.

Ronald P. Lepping received the B.S. degree from Villanova University, the M.S. degree from Drexel, and the Ph.D. degree from Rensselaer Polytechnic Institute.

He is a space scientist at the NASA Goddard Space Flight Center. He is the principal investigator of the IMP-8 and WIND magnetometers and a co-investigator on the Voyager magnetometer experiment.

In 1991, he was awarded the NASA medal of exceptional scientific achievement for his studies on planetary magnetospheres and the interplanetary medium.

James B. Byrnes received the B.S. degree in mathematics from St. Mary's College and the M.S. degree in numerical science at Johns Hopkins.

He is a mathematican at the NASA Goddard Space Flight Center. He has been at the center since 1980 and has been involved in the processing and analysis of data products from many scientific spacecraft, including the Dynamics Explorer and GEOTAIL probes. His research interests include numerical analysis, computer systems design, and custom-tailored application software.